Spatially and Temporally Modulated Traveling-Wave Pattern in Convecting Binary Mixtures

Jay Fineberg,[1] Elisha Moses,[1] and Victor Steinberg[1,2]

[1]*Department of Nuclear Physics, Weizmann Institute of Science, Rehovot, 76100, Israel*

[2]*Center for Nonlinear Studies, Los Alamos National Laboratory, Los Alamos, New Mexico 87545*

(Received 10 February 1988)

A new state composed of quasiperiodic traveling waves has been observed in very close vicinity of the convection onset along a stable branch. This state precedes the recently discovered confined traveling-wave state, and consists of left- and right-going traveling waves which periodically alternate between either side of the cell. A time-dependent wave-number spectrum is a characteristic feature of this pattern. Effects of pattern translation and modulational instability can qualitatively explain the observed dynamical behavior.

PACS numbers: 47.25.−c

The recent observation of traveling waves (TW) in convecting binary mixtures in a finite-size container provides the opportunity to perform well-controlled experiments on properties that characterize a wide class of open systems. Well-known examples are free shear flows (wakes, jets, mixing layers), plane Poiseuille and pipe flows, drift waves in plasmas, etc.[1,2] In most of these cases the generalized Ginzburg-Landau (GGL) equation can be derived as a simple model to describe the nonlinear evolution of propagating patterns.[2]

A distinct feature of these systems is that a single nondimensional parameter, s^*, determines whether they are convectively or absolutely unstable, thereby determining their spatial pattern as well as their temporal behavior. This parameter is the ratio of the group velocity of a wave packet, s, to the local growth rate, τ^{-1}, on the characteristic length scale ξ, so that in the framework of the GGL equation,[1-3] $s^* = s\tau/(\xi\epsilon^{1/2})$, where ϵ is the control parameter. [$\epsilon = (R - R_c)/R_c$, R, is the Rayleigh number, and R_c is its value at the convection threshold.] Cross[4,5] has recently performed numerical simulations of the nonlinear coupled GGL equations with real coefficients for left and right propagating waves for a binary mixture in a finite container. Taking into account only the effects of pattern propagation, Cross showed that, similar to open systems, the same parameter s^* determines the relation between convected and absolutely unstable conditions and thereby the selected pattern of the system. An astonishing fact is that the rich variety of TW patterns predicted by the simulations have been independently observed experimentally: full-cell nonlinear TW,[6,7] spatially modulated TW (confined TW)[7,8] and nonlinear counterpropagating waves (CPW).[7]

An effect of the complex coefficients in the GGL on convectively unstable solutions is that the selected wave number k^* behind a front may become unstable to modulational (or Benjamin-Feir) instability, even though a band of stable wave numbers exists.[2] If k^* is selected outside of this stable band, it would lead to time-dependent behavior in the k spectrum.[9]

In this Letter we report our observation of a new nonlinear spatially and temporally modulated TW pattern which was also observed independently in the numerical simulations.[5] This TW pattern, coined by us as a "blinking state," was observed in very close vicinity of the convection threshold, and it precedes the recently discovered confined TW.[7,8] The general importance of the observations reported is twofold in light of the ideas described above. First, this TW state is closely related to the linear oscillatory state due both to the small deviations of the blinking-state frequency from the neutral frequency, f_0, of the linear state and to its relatively small amplitude. It means that the linear concentration gradient is perturbed slightly, and thus this state can be quantitatively described by the GGL equation. However, both linear and weakly nonlinear TW states behave differently with respect to mass transport. As our recent experiment shows[10] subcritical bifurcation to a weakly nonlinear state coincides with the mass-transport onset which modifies the linear concentration profile. Second, the observed time-dependent wave-number spectrum of the blinking state appears to be related to the modulational instability mentioned above. Thus, for the first time the effects of this mechanism are observed in a driven nonequilibrium system.

In a binary fluid, the parameters which determine the convective flow are R, which is proportional to the temperature difference across the fluid layer, ΔT, and the separation ratio, ψ, which is a measure of the coupling between the temperature and concentration gradient, induced by the Soret effect.[11] For $\psi < 0$, the concentration gradient stabilizes the quiescent state and leads to an oscillatory instability.[11] Other relevant parameters are the Prandtl number, $P = \nu/\kappa$, and the Lewis number, $L = D/\kappa$, where ν is the kinematic viscosity, and D and κ are the mass and thermal diffusivities, respectively.

The experiments were done on ethanol-water mixtures with weight concentrations of ethanol in the range between 26% and 28.5% at 31 °C mean temperature ($-0.058 \leq \psi \leq -0.005$, $P = 18$, $L = 0.012$), and a ben-

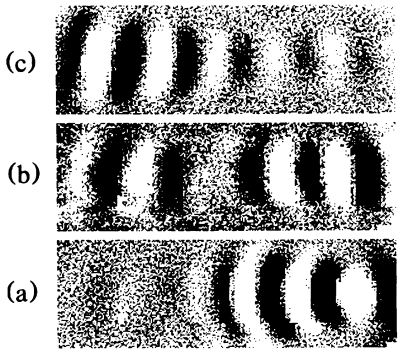

FIG. 1. Representative shadowgraph images of the blinking TW state for $\psi=-0.045$ in benzene methanol. (a) Right TW; (b) convection in both sides of the cell; (c) left TW.

zene-methanol mixture with a 95% by weight concentration of benzene at 30.2°C ($\psi=-0.045$, $P=7.5$, $L=0.025$). Cells were used having nearly 1D geometries and various aspect ratios 1:4:Γ, where Γ ranges from 12 to 12.7, as well as 20 and 27 (with height $d=0.305$ cm). The apparatus, described elsewhere,[7,8] enabled us to make both high-resolution heat-flow (Nusselt number) as well as precision shadowgraph measurements.

Figure 1 shows computer-enhanced shadowgraph images of the blinking TW state with time at three moments during one period of the modulation. Details of the state's dynamics are presented by contour plots in Fig. 2. At the beginning of the modulation period this TW state is confined to one side of the cell, propagating in the direction of a lateral wall [Fig. 2(a)]. Then it starts to fade as another TW propagating in the opposite direction appears [Fig. 2(b)], and, finally, the amplitude of the TW propagating in the opposite direction grows while the TW amplitude on the other side decays completely [Fig. 2(c)]. This cycle then repeats itself.

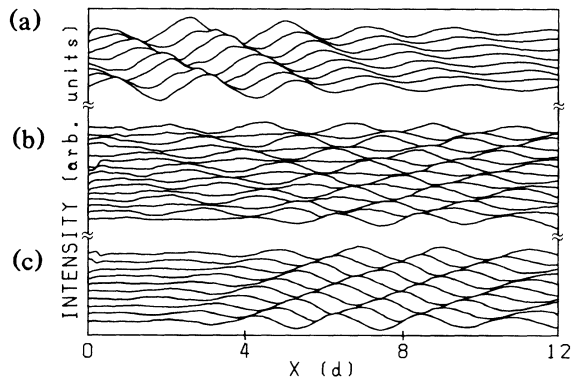

FIG. 2. Contour plot of shadowgraph signals for the blinking TW state taken at $\epsilon=0.0048$ with $\psi=-0.014$ in ethanol water as a function of position along the cell length at time intervals of $0.66t_v$. Time increases upwards. They are taken at the following times: (a) $106t_v$; (b) $66t_v$; (c) $0t_v$ (cycle time = $198t_v$, $t_v=90.6$ s).

Nusselt number (N) versus ϵ measurements of three different convective states are shown in close vicinity of the convective threshold [Fig. 3(a)] for the ethanol-water mixture at $\psi=-0.014$. For a small step from the conduction state ($\epsilon\leq 0.002$), a hysteretic transition to the blinking state occurs with a discontinuous change in N on the order of 0.1%. This transition appears by way of transient linear CPW[12] with the observed frequency $\omega_0=2\pi f_0 t_v=2.505$ which is close to the calculated value of $\omega_0=2.5$. ($t_v=d^2/\kappa=90.6$ s is the vertical diffusion time.) The blinking state persists along the nonlinear branch (region I) for a range of about $\Delta T=10$ mK ($\Delta\epsilon\approx 0.006$) until a continuous transition in heat transport to confined TW occurs (region II). Time dependence in heat transport due to the amplitude modulation in region I was reduced by averaging over several hours, although large scatter in the data remains. Stable nonlinear CPW were observed on cooling in a hysteretic region III. The TW frequencies corresponding to the Nusselt number data are shown at the top of Fig. 3(a). In region I the basic frequency ω_1 of the blinking TW is nearly constant over $\Delta\epsilon\approx 0.0035$ and is within 10%–15% of the value of ω_0. In addition ω_1 closely fol-

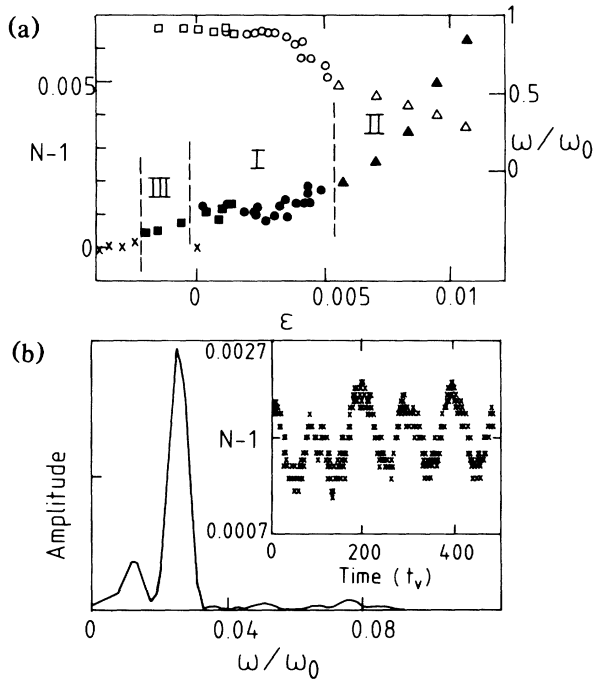

FIG. 3. (a) Steady-state Nusselt number, N, and scaled TW frequency ω_1/ω_0 as a function of ϵ. Vertical lines define regions of different nonlinear TW patterns: (I) blinking TW pattern (circles); (II) confined TW state (triangles); (III) hysteretic region with stable nonlinear CPW patterns (squares). Crosses show the conduction state. N and ω_1/ω_0 are shown by full and empty symbols, respectively. (b) N for the blinking state (region I) as a function of time and its spectrum at $\epsilon=0.0034$ with $\psi=-0.014$ in ethanol-water mixture.

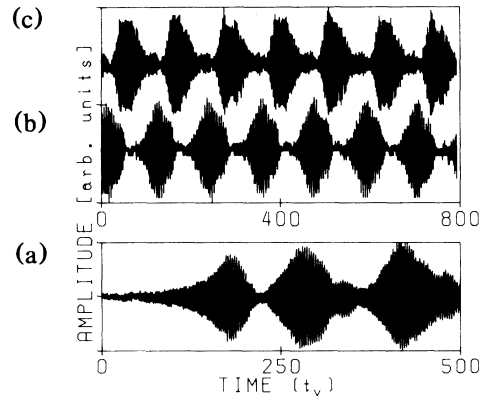

FIG. 4. (a) Intensity of the shadowgraph signal at one point as a function of time as ϵ increases from conduction to a value of $\epsilon=0.0009$ at $\psi=-0.014$. Several cycles of the blinking TW state (steady state) at $\epsilon=2\times10^{-4}$ with $\psi=-0.020$: (b) signal taken at one point on the left side of the cell; (c) signal taken concurrently at a point on the right side of the cell.

lows changes in N over the entire branch. The time-dependent part of N for the blinking state is presented in the inset of Fig. 3(b). The corresponding power spectrum shows a sharp peak at the slow modulation frequency $\omega_2=0.02\omega_0$.

Figure 4 demonstrates the time-dependent behavior of the blinking state by the intensity measured at one point of the shadowgraph image. As ϵ increases above threshold, the oscillation amplitude grows exponentially. This transient linear CPW reaches saturation as the state's amplitude becomes temporally modulated [Fig. 4(a)]. Figures 4(b) and 4(c) show several modulation cycles of the blinking state in a steady-state region (after the transient decays) for the ethanol-water mixture. The frequency of the modulation is nearly constant and much lower than that of the TW. This steady-state scenario is reached after relaxation times on the order of several horizontal diffusion times which for the longer cell can reach 30–40 h.

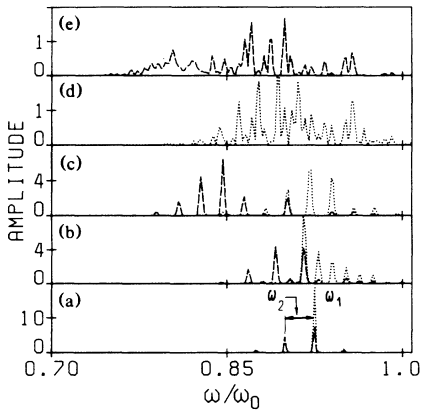

FIG. 5. Power spectra of the shadowgraph signal for the blinking TW patterns taken at points situated at each end of the cell. Dotted line: spectra taken at a point situated on the right side of the cell. Dashed line: spectra taken at a point situated on the left side of the cell. All spectra shown were taken at $\psi=-0.020$. (a) $\epsilon=-1.3\times10^{-3}$, (b) $\epsilon=-8.5\times10^{-4}$, (c) $\epsilon=1.5\times10^{-4}$, (d),(e) $\epsilon=7\times10^{-4}$. Basic ω_1 and modulation ω_2 frequencies are labeled on the graph.

Power spectra of the shadowgraph signal intensity taken at points situated at opposite sides of the cell during the blinking state are shown in Fig. 5. The spectra low on the branch are quasiperiodic indicating a two-frequency state. The peak separation is discrete and corresponds to the blinking frequency ω_2. All peaks in the spectrum can be given as an integer combination of two neighboring peaks. Very low on the branch [Figs. 5(a) and 5(b)], the main peak at ω_1 is identical on both sides of the cell. Higher up on the branch [Fig. 5(c)], the main peaks at the cell's ends separate. Each spectrum in turn remains quasiperiodic. The lower and higher parts of the spectra are not shown since their amplitudes are several orders of magnitude smaller than the spectra shown. Still higher on the branch [Figs. 5(d) and 5(c)], the spectra become more complicated but are still discrete as the simple two-frequency quasiperiodic state evolves into one more complex. The process ends at a continuous transition to the confined-state branch. At this point the power spectrum narrows to a single sharp peak.

Dimensional analysis of these spectra shows that the correlation dimension D jumps from $D\approx2$ for the simple two-frequency state to $D\leq3$ for the more complicated state. The latter suggests that this more complex but still discrete spectrum corresponds to a three-frequency quasiperiodic state observed in recent simulations.[13]

One of the most striking features of the blinking state is the variation of the wave number in time during the modulation period. Time-dependent wave-number spec-

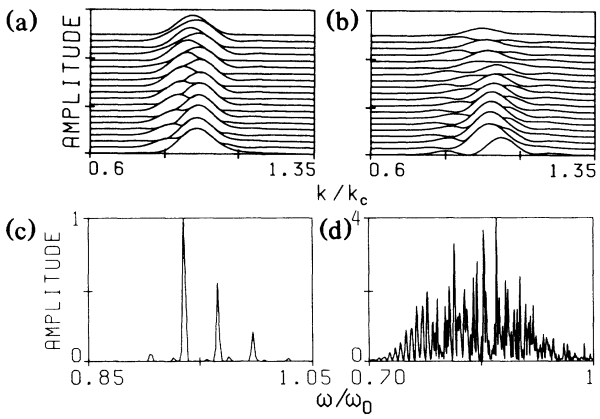

FIG. 6. (a),(b) Wave-number spectra of blinking TW pattern at consecutive time intervals $0.32t_v$ at (a) $\epsilon=1.5\times10^{-3}$ and (b) $\epsilon=3\times10^{-3}$ for $\psi=-0.058$. (c),(d) Power spectra corresponding to (a) and (b), respectively.

tra are shown in Fig. 6. Each line on the plot represents the power spectrum in k space of the optical signal at one moment. The time interval between lines is $0.32t_v$. It is clearly seen that the wave number of the blinking state never settles down to a steady-state value. In the simple two-frequency quasiperiodic case shown in [Figs. 6(a) and 6(b)], the state oscillates between two wave numbers whose difference, Δk, can be estimated as $\Delta\omega(d\omega/dk)^{-1}=0.055$. This can be compared to the modulationally stable wave-number band[14] which for $\epsilon=0.0015$ is $\Delta k_{st}\approx 0.05$, i.e., the wave number selected by the blinking state appears outside of the modulationally stable wave-number band. A possible explanation for the time-dependent wave-number spectra of the state may lie in the interplay between two mechanisms: One is the selection mechanism of the convectively unstable blinking state and the other is the modulational instability of TW as discussed previously. More complicated time dependence of the wave-number spectrum for $\epsilon=0.003$ is shown in Fig. 6(b). This state corresponds to a three-frequency quasiperiodic state [Fig. 6(d)].

Thus, we have presented experimental results on a weakly nonlinear TW state whose amplitude is spatially and temporally modulated.[15] Numerical simulations carried out by Cross[5] show that at $s^*>2$ the confined TW solution becomes unstable to periodic modulation. The corresponding modulated TW pattern shown in the simulations qualitatively reproduces the main features of the blinking state.[5] Our estimates verify that all blinking states were observed at $s^*>2$. However, the time-dependent k spectrum cannot be explained merely by the combination of propagation and finite geometry, and the full complex GGL equation is needed to describe it.

We are grateful to I. Procaccia and A. Newell for helpful and stimulating discussions. This work was supported in part by the U.S.-Israel Binational Science Foundation Grant No. 8400256, and the Minerva Foundation.

[1]J. M. Chomaz, P. Huerre, and L. G. Redekopp, Phys. Rev. Lett. **60**, 25 (1988); G. S. Triantafyllou, K. Kupfer, and A. Bers, Phys. Rev. Lett. **59**, 1914 (1987), and references cited therein.

[2]K. Nozaki and N. Bekki, Phys. Rev. Lett. **51**, 2171 (1983).

[3]P. Huerre, in *Instabilities and Nonequilibrium Structures,* edited by E. Tirapegi and D. Villarroel (Reidel, Dordrecht, 1987), p. 141.

[4]M. Cross, Phys. Rev. Lett. **57**, 2935 (1987).

[5]M. Cross, to be published.

[6]R. W. Walden, P. Kolodner, A. Passner, and C. Surko, Phys. Rev. Lett. **55**, 496 (1985).

[7]E. Moses and V. Steinberg, Phys. Rev. A **34**, 693 (1986), and Nucl. Phys., Proc. Suppl., **B2**, 109 (1987).

[8]E. Moses, J. Fineberg, and V. Steinberg, Phys. Rev. A **35**, 2757 (1987); R. Heinrichs, G. Ahlers, and D. S. Cannell, Phys. Rev. A **35**, 2761 (1987).

[9]A. Newell, private communication. One of us (V.S.) is grateful to A. Newell for clarifying this point.

[10]E. Moses and V. Steinberg, Phys. Rev. Lett. **60**, 2030 (1988), and to be published.

[11]D. T. J. Hurle and F. Jakeman, J. Fluid Mech. **47**, 667 (1971); V. Steinberg, J. Appl. Math. Mech. **35**, 335 (1971).

[12]P. Kolodner, A. Passner, C. Surko, and R. Walden, Phys. Rev. Lett. **56**, 2621 (1986).

[13]M. Bestehorn, R. Friedrich, and H. Haken, to be published.

[14]J. T. Stuart and R. C. DiPrima, Proc. Roy. Soc. London A **362**, 27 (1978).

[15]After submission of this manuscript, we received a paper from P. Kolodner and C. Surko, following Letter [Phys. Rev. Lett. **61**, 842 (1988)], describing related observations.

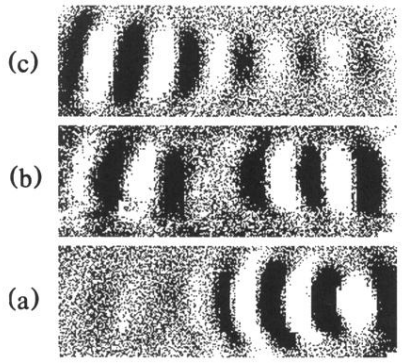

FIG. 1. Representative shadowgraph images of the blinking TW state for $\psi = -0.045$ in benzene methanol. (a) Right TW; (b) convection in both sides of the cell; (c) left TW.

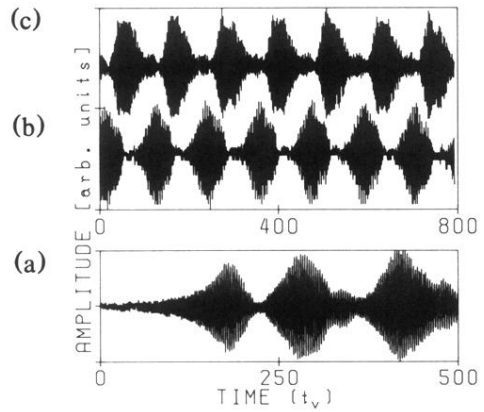

FIG. 4. (a) Intensity of the shadowgraph signal at one point as a function of time as ϵ increases from conduction to a value of $\epsilon=0.0009$ at $\psi=-0.014$. Several cycles of the blinking TW state (steady state) at $\epsilon=2\times10^{-4}$ with $\psi=-0.020$: (b) signal taken at one point on the left side of the cell; (c) signal taken concurrently at a point on the right side of the cell.